Volume 16 No.1
January 2024
ISSN : 2085 – 1669
e-ISSN : 2460 – 0288
Website : jurnal.umj.ac.id/index.php/jurtek
Email : jurnalteknologi@umj.ac.id

Jurnal Teknologi
UNIVERSITAS MUHAMMADIYAH JAKARTA

# Slope Stability Evaluation and Geometrical Recommendation Using The Morgenstern Price Method

**Heri Matius Sesa[1], Najib[2*], Hasnan Luthfi Dalimunthe[3], Zerlinda Handietri[4]**
[1,2,3]*Departemen Teknik Geologi, Fakultas Teknik, Universitas Diponegoro, Jl. Prof. Soedarto, SH., Tembalang, Kota Semarang, 50275*
[4]*PT Indocement Tunggal Prakarsa Tbk., Plant Palimanan*
*Corresponding author: najib@ft.undip.ac.id

**Jurnal Teknologi use only:**
Received 26 July 2023; Revised 12 September 2023; Accepted 28 September 2023

**ABSTRACT**

The study is located on PT Indocement Tunggal Prakarsa Tbk., which is still actively engaged in mining operations. The study aimed to determine the slope Safety Factor (SF) and offer suggestions for safe slope geometry for mining operations. Primary data collection through observation of lithology conditions, sample testing in the laboratory, scanline mapping, slope geometry measurements, and secondary data obtained from company inventories and related sources. The kinematic approach is used to assess the risk of landslides. This slope stability study uses boundary equilibrium based on the Morgenstern Price and Mohr-Coulomb failure criteria. Limestone is the majority of the rocks in the location. The kinematic analysis demonstrated that direct toppling and wedge toppling are the landslide potential at the research location. Using the non-circular boundary equilibrium approach, slope stability analysis was carried out on four Regions with dry and saturated groundwater conditions i.e, Regions A', B140, C120, and C135. The four Regions have stable slopes and are in good condition (SF values over 1.25). For the excavation to be carried out optimally, the recommendations for optimization of the overall slope geometry are given, namely, the height of the bench is 10 m, and the width of the ladder is 4 m. The slope angle is $80^{o}$, with SF value of 3.035 in dry conditions and an SF value of 2.021 in saturated conditions.

**Keywords**: Slope Stability, Limestone Quarry, Landslide Potential, Factor of Safety

## Introduction

One of the major sectors that contributes to Indonesia's development is the cement industry. Limestone is one of the raw minerals required in cement production. Calcium carbonate, or CaCO3, forms more than 50% of limestone [1-2]. 28.7 billion tonnes of limestone have been discovered in Indonesia [3]. Open-pit mining is the most common method to extract limestone [4].

Drilling, blasting, material extraction, and transportation are all potential contributors to air pollution in open-pit mining [5-6]. Drilling and blasting operations have the potential to generate air pollution. Blasting can also degenerate the rock mass condition by establishing a network of internal smooth fractures that impact the slope's stability and safety [7].

Indocement Tunggal Prakarsa Tbk is a mining company of limestone that has been practiced for many years. The mining method is quarry mining, which is an open-pit mining system. The mine slopes could become increasingly steeper due to the mining activity. Slope stabilization operations are necessary for unstable slope situations to ensure worker safety and the business's financial sustainability. Slope failure in limestone mines has happened several times, including in Japan. In the Kagemoro limestone mining area, there was a collapse of limestone material in 1973 that led to the loss of more than 300,000 $m^3$ of material altogether [8].

DOI: https://dx.doi.org/10.24853/jurtek.16.1.53-64

ISSN : 2085 – 1669
e-ISSN : 2460 – 0288

Slope design in open-pit mines is a challenge that must be managed appropriately since ongoing mining operations will significantly impact it and affect equipment safety, worker safety, property, and production efficiency [9]. Thus, an assessment of slope stability of existing slopes is required. The existence of discontinuity regions is one of many factors that could influence a slope's stability [10-11].

Analyzing slope stability in the geotechnical sector has been widely practiced, applying numerical computation methods [12-18]. Other methods for the examination of rock masses, such as the RMR (Rock Mass Rating) from [19] and the SMR (Slope Mass Rating) from [20], are also implemented. By evaluating geomechanical parameters, shear strength, slope morphometry, and rock mass characteristics, This method is helpful to determine whether rock slopes are stable[21], RMR and modified SMR were used by [22] to do a three-dimensional analysis of the stability of open-pit mining slopes.RMR and SMR data were employed by [23] in their investigation of slope stability in tropical regions and volcanoes.

The probability of landslides in limestone mines has been the subject of a significant amount of research, including [24] analysis of potential landslides in mines using the Open PIT system operated by PT Holcim Indonesia Tbk, which is located in Cileungsi District, Bogor Regency, West Java. Kinematic analysis is a technique used in previous studies, and the findings demonstrate that toppling and wedge landslides occur. Using the kinematic method, [25] assessed the likelihood of landslides on limestone quarry slopes in the Bogor region. The results of this study show there is a possibility that wedge and plane landslides might occur.

The investigation will examine the rock mass in four Regions of PT mining slopes. Indocement Tunggal Prakarsa Tbk uses RMR, GSI, and SMR analyses. Furthermore, kinematic analysis and landslide potential evaluation were performed. Following this research, recommendations regarding slope geometry and slope stability analysis are presented. The analyses above are utilized to assess the stability of slopes at mining sites. This research will provide information regarding slope stability conditions and safety factor values. If the slope stability analysis finds a relatively high FS (Safety Factor) value, then slope-cutting optimization can be carried out close to the critical limit. In order to obtain limestone in the most effective, efficient, and secure manner possible, slope cutting has been optimized. This study aims to provide broad audiences with more information on slope stability and to be used as a model to develop a slope's geometry.

## Methods

Primary Data Collection

Geological mapping was used to observe lithological conditions and technical geological conditions, such as weathering levels and geological structures, as well as to collect primary data. Rock samples were also gathered at the research location within the mining IUP (mining license) limits of the research area. The next step is scanline mapping, which involves collecting data on every geological structure and discontinuity region (rock discontinuities) that crosses or intersects the scan line. [26] states that the sample line is 10 to 50 times longer than the typical distance between discontinuities.

Afterward, measurements of the scanline orientation and discontinuity orientation take place alongside measurements of the weathering level, the discontinuity areas' roughness, the discontinuity openings' width, the spacing between the discontinuities, and the groundwater condition in the rock Region. They utilize nails, a penknife, and a geological hammer to obtain rock samples at the discontinuity location to assess the compressive strength of the intact rock. Subsequently, the samples are analyzed in a lab. The following step is to measure the actual slope geometry using an application named Avenza Maps, a geological compass, and a rolling rule. The measurements were performed using a geological compass to measure each level's slope angle and a tape measure to determine each level's length and width. Laboratory tests are conducted on rock samples gathered during fieldwork to identify the rock compressive strength test results.

Secondary Data Collection

The shapefile (SHP) of the mining IUP area of the research area, the geological map of the

Jurnal Teknologi 16 (1) pp 53-64 © 2024

research area, the PGA Map obtained from [27], and standard vibration levels blasting following company standards based on the reference SNI 7571 of 2010 [28] are secondary data used in this research. As suggested by [29], the Earthquake Hazard Map Indonesia 2017 reference (SPGA) and amplification factors for PGA (FPGA) (Figure 1) can be employed to multiply the PGA value in the bedrock (SB) (Table 1) by the PGA value at the surface of the ground based on site (PGAM).

**Table 1.** Amplification factors for PGA (FPGA) [27].

| *Site Classification* | SPGA | | | | |
|---|---|---|---|---|---|
| | **PGA ≤ 0,1** | **PGA =0,2** | **PGA =0,3** | **PGA=0,4** | **PGA ≥0,5** |
| Hard Rock ($S_A$) | 0,8 | 0,8 | 0,8 | 0,8 | 0,8 |
| Rock ($S_B$) | 1 | 1 | | 1 | 1 |
| Very Dence Soil and Soft Rock ($S_C$) | 1,2 | 1,2 | 1,1 | 1 | 1 |
| Medium Soil ($S_D$) | 1,6 | 1,4 | 1,2 | 1,1 | 1 |
| Soft Soil ($S_E$) | 2,5 | 1,7 | 1,2 | 0,9 | 0,9 |
| Special Soil ($S_F$) | SS | SS | SS | SS | SS |

$$PGA_M = F_{PGA} \times S_{PGA} \quad (1)$$

FPGA = 0,15
SPGA = 1
PGAM = FPGA x SPGA
= 0,15 x 1
= 0,15g

Data Processing

Following data collection, processing of the data is completed, including calculating the actual discontinuity distance/spacing, RQD value, weighting the RMR value, GSI value, SMR value, determining landslide potential using the kinematic method, cohesion value, internal shear angle value, calculating the value of the slope stability, and evaluating SF results. To determine the rock's strength and quality mass as well as slope stability conditions, the rock mass is determined through SMR and RMR. Likewise, understanding the slope material's characteristics becomes essential for slope stability analysis. The category of failure criterion that will be applied in this research depends on the type of material used [30].

Data Analysis

The slope safety factor's value is to be verified by slope stability analysis. Non-circular analysis is applied in processing utilizing the Morgenstern Price method; this is a surface area analysis that evaluates the circumstances of a single encounter with landslide-type scenarios. The wedge sliding and direct toppling types of landslides are the possible forms that might occur. Slope height, slope orientation, dip and strike, seismic values, groundwater conditions, and other disturbances constitute some of the criteria that are taken into the SF analysis [31].

The first step in the analysis stage is building up the real slope geometry or actual circumstances. The Mohr-Coulomb input parameter values should be filled in after constructing a lithology layer based on the results of field observations. These variables are rock density, internal friction angle, and cohesiveness value. The maximum Ground Peak Acceleration (PGA) value over earthquakes is another considered measure. Furthermore, there are presumptions concerning the existence of groundwater in dry and wet conditions. The results of this research will provide data on the slope safety factor's value, which can be used as a basis or point of reference for proposals for the final slope geometry design.

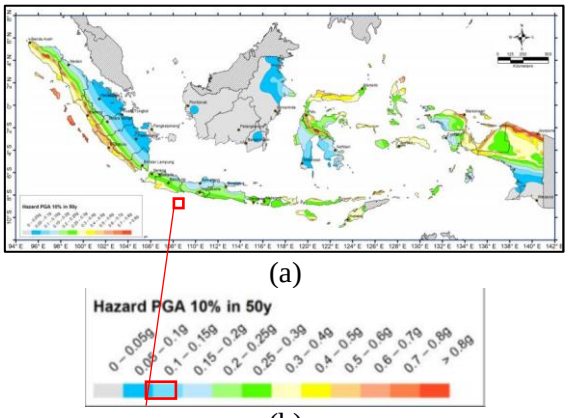


(a)

(b)

**Figure 1.** PGA map in bedrock for 10% exceedance probability in 50 years (a) and enlargement of the legend [27]**.**

1. Laubsher, 1975

| SMR | RMR |
|---|---|
| 75$^o$ | 81 - 100 |
| 65$^o$ | 61 - 80 |
| 55$^o$ | 41 - 60 |
| 45$^o$ | 21 - 40 |
| 35$^o$ | 0 - 20 |

2. Hall, 1985

$$SMR = 0,65\ RMR + 25 \quad (2)$$

ISSN : 2085 – 1669
e-ISSN : 2460 – 0288

3. Orr,1992
   SMR = 35 ln RMR – 71 (3)

**Results and Discussions**

Scanline Mapping

Region A'

Sixteen discontinuity regions were discovered in region A' applying slope and scanline orientation data (Table 2). A rough discontinuity area in Region A has been filled with weathered material, primarily mudstone, and has slightly weathered weathering conditions (Figure 3).

**Table 2.** Orientation of scanline and slopes on Region A'

| Information | Value |
|---|---|
| Slope Height | 7 m |
| Slope Width | 35 m |
| Slope (Strike) | 281° |
| Slope Dip | 75° |
| Scanline Length | 20 m |
| Scanline (Strike) | 102° |
| Scanline Dip | 4° |


**Figure 3.** Slope conditions for scanline data in Region A', with the yellow line indicating the length of the scanline.

Region B140

Slope and scanline orientation data were used to identify 10 discontinuity locations in Region B140 (Table 3). It has a discontinuity region in Region B140 with a rough surface condition, no material to fill the gaps of the discontinuity area, and a mildly worn weathering level (Figure 4).

**Table 3.** Orientation of scanline and slopes on region B140

| Information | Value |
|---|---|
| Slope Height | 10 m |
| Slope Width | 22,5 m |
| Slope (Strike) | 2° |
| Slope Dip | 83° |
| Scanline Length | 11,5 m |
| Scanline (Strike) | 350° |
| Scanline Dip | 50° |

Region C120

Using slope and scanline orientation information, 19 discontinuity locations in Region C120 were identified (Table 4). It is a discontinuity region with a rough surface condition in Region C120, no material used to fill in the gaps, and a gently weathered weathering level (Figure 5).


**Figure 4.** Slope conditions for scanline data in Region B140, with the yellow line indicating the length of the scanline.

**Table 4.** Orientation of scanline and slopes on Region C120

| Information | Value |
|---|---|
| Slope Height | 15 m |
| Slope Width | 15 m |
| Slope (Strike) | 9° |
| Slope Dip | 86° |
| Scanline Length | 15 m |
| Scanline (Strike) | 352° |
| Scanline Dip | 7° |

Region C135

Sixteen discontinuity areas were found with slope and scanline orientation data in Region C135 (Table 5). In the gaps of the discontinuity area, filling material in the form of weathered material, particularly mudstone, and slightly weathered weathering conditions have been identified (Figure 6).

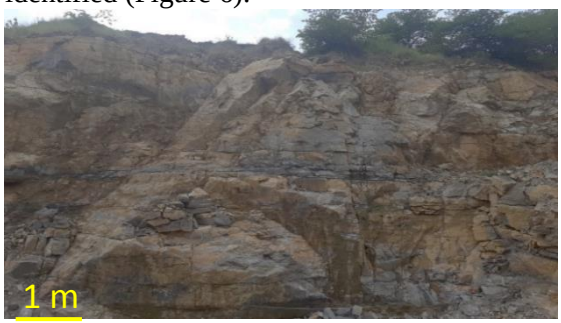


**Figure 5.** Slope conditions for scanline data in Region C120, with the yellow line indicating the length of the scanline.

Jurnal Teknologi 16 (1) pp 53-64 © 2024

**Table 5.** Orientation of scanline and slopes on Region C135

| Information | Value |
|---|---|
| Slope Height | 10 m |
| Slope Width | 18 m |
| Slope (Strike) | 247° |
| Slope Dip | 80° |
| Scanline Length | 13 m |
| Scanline (Strike) | 270° |
| Scanline Dip | 2° |

Rock Mass Classification

Rock Quality Designation (RQD)

According to [32], the Rock Quality Designation (RQD) value in the study region exhibits extremely high overall results, with an average of 99.870%, included in the excellent classification. The small number of or frequent discontinuity spots in the rock mass at the subject of the investigation site impacts the high RQD value. This indicates that the fewer joints or discontinuity zones, the higher the rock mass quality. As stated by [33], the greater the rock quality, the greater the rock mass's RMR value. The possibility for pore opening or groundwater saturation will be larger if the RQD value is lower since the current rock will be less intact, and the strength will decrease substantially [34].


**Figure 6.** Slope conditions for scanline data in Region C135, with the yellow line indicating the length of the scanline.

Rock Mass Rating (RMR)

Based on the RMR weighting data, it was found that Region A', B140, C120, and C135 have an average value of RMR 65, 73,73, and 67, respectively (Table 6-9)). [19] states that the value of RMR is 76.333, categorized as good rock mass (class II), as shown in Table 10. According to [19], the RMR value in class II indicates internal friction with an angle ranging from 35° to 45° and cohesiveness between 300 kPa and 400 kPa. High cohesion and internal friction angle values impact stabilizing the slope.

**Table 6.** RMR value on Region A.'

| Rock Mass Rating [19] | | | | |
|---|---|---|---|---|
| **Parameter** | **Information** | | | **Value** |
| Fracture strength of Intact Rock | 17,54 | | | 2 |
| RQD | 99,789 | | | 20 |
| Discontinuity Spacing | 1,503 | | | 15 |
| Discontinuity Conditions | Roughness | Rough | 5 | 18 |
| | Gap | 1-5 mm | 1 | |
| | Filler Material | Clay | 3 | |
| | Weathering | Moderately | 5 | |
| | Continuity | 1-3 m | 4 | |
| Groundwater | Moist | | | 10 |
| **TOTAL VALUE** | | | | 65 |

**Table 7.** RMR value on Region B140

| Rock Mass Rating [19] | | | | |
|---|---|---|---|---|
| **Parameter** | **Information** | | | **Value** |
| Fracture strength of Intact Rock | 52,36 | | | 7 |
| RQD | 99,865 | | | 20 |
| Discontinuity Spacing | 1,890 | | | 15 |
| Discontinuity Conditions | Roughness | Rough | 5 | 21 |
| | Gap | 1-5 mm | 1 | |
| | Filler Material | No | 6 | |
| | Weathering | Moderately | 5 | |
| | Continuity | 1-3 m | 4 | |
| Groundwater | Moist | | | 10 |
| **TOTAL VALUE** | | | | 73 |

**Table 8.** RMR value on Region C120

| Rock Mass Rating [19] | | | | |
|---|---|---|---|---|
| **Parameter** | **Information** | | | **Value** |
| Fracture strength of Intact Rock | 16,81 | | | 2 |
| RQD | 99,961 | | | 20 |
| Discontinuity Spacing | 3,515 | | | 20 |
| Discontinuity Conditions | Roughness | Rough | 5 | 21 |
| | Gap | 1-5 mm | 1 | |
| | Filler Material | Clay | 6 | |
| | Weathering | Moderately | 5 | |
| | Continuity | 1-3 m | 4 | |
| Groundwater | Moist | | | 10 |
| **TOTAL VALUE** | | | | 73 |

**Table 9.** RMR value on Region C135

| Rock Mass Rating [19] | | |
|---|---|---|
| **Parameter** | **Information** | **Value** |
| Fracture strength of | 26,99 | 4 |

ISSN : 2085 – 1669
e-ISSN : 2460 – 0288

| | | | | |
|---|---|---|---|---|
| Intact Rock | | | | |
| RQD | 99,865 | | | 20 |
| Discontinuity Spacing | 1,888 | | | 15 |
| Discontinuity Conditions | Roughness | Rough | 5 | 18 |
| | Gap | 1-5 mm | 1 | |
| | Filler Material | No | 3 | |
| | Weathering | Moderately | 5 | |
| | Continuity | 1-3 m | 4 | |
| Groundwater | Moist | | | 10 |
| **TOTAL VALUE** | | | | 67 |

**Table 10.** Meaning of rock mass classes on all study area Regions based on RMR value **[19].**

| **Class number** | **I** | **II** | **III** | **IV** | **V** |
|---|---|---|---|---|---|
| *Average stand-up time* and spam | 20 years, 15 m | 1 year, 10 m | 1 week, 5 m | 10 hours, 2,5 m | 30 minute , 1 m |
| Rock mass cohesion | > 400 kPa | 300 - 400 kPa | 200 - 300 kPa | 100 - 200 kPa | < 100 kPa |
| Internal shear angle | > 45$^{o}$ | 35$^{o}$ - 45$^{o}$ | 25$^{o}$ - 35$^{o}$ | 15$^{o}$ - 25$^{o}$ | < 15$^{o}$ |

Geological Strenght Index (GSI)
The results of the GSI values in the rock masses of Regions A', B140, C120, and C135 based on the RMR values obtained have an average GSI value of 64.5 as presented in Table 11, which is obtained from the RMR value minus 5 according to [35], demonstrating that e rock mass quality belongs to a good category(Figure 7).

The obtained GSI value is included in the high-quality rock mass condition, and the rock mass has been described as having a Regiony state in which the rock mass has been affected by discontinuity areas formed by three or more joint sets and has a good surface condition. This might indicate a possibility of geotechnical hazards in the form of structural collapse in the study area due to discontinuities, which decrease the strength of the rock mass [36].

**Table 11.** GSI Value of the Research Area

| Region | RMR | GSI |
|---|---|---|
| A' | 65 | 60 |
| B140 | 73 | 68 |
| C120 | 73 | 68 |
| C135 | 67 | 62 |
| Average of GSI value | | 64.5 |

Slope Mass Rating (SMR)
In order to determine the suggested slope angle for stable stripping slopes in the study area, the SMR value is determined for each slope, namely areas A', B140, C120, and C135. The average SMR value is calculated from the four slope areas (Table 12). Three SMR classes are applied in the SMR value calculation to determine the greatest slope angle. The proposed slope angle for mining optimum in the study region will employ this SMR value for the opening angle.

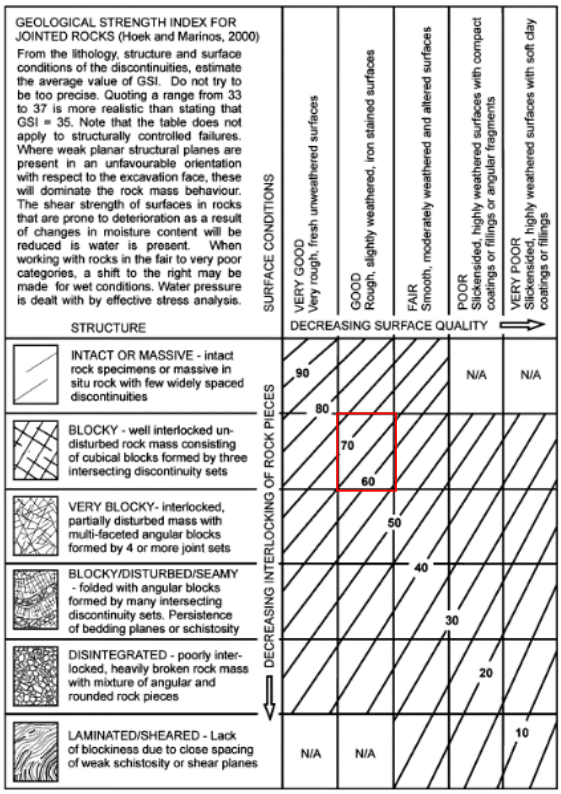


**Figure 7.** The GSI value classification graphic shows that the rock mass's quality was assessed as excellent, as indicated by the red box [35].

**Table 12.** SMR Value of the Research Area

| **Classification** | **SMR (º)** | | | | **Average (º)** |
|---|---|---|---|---|---|
| | **A'** | **B140** | **C120** | **C135** | |
| Laubscher (1975) | 65 | 65 | 65 | 65 | 65 |
| Hall (1985) | 67,25 | 72,45 | 72,45 | 68,55 | 70,16 |
| Orr (1992) | 75,1 | 79,17 | 79,17 | 76,16 | 77,4 |

Jurnal Teknologi 16 (1) pp 53-64 © 2024

Landslide Potential

Using the software program Dips 6.0, the landslide potential in the study region was analyzed. The results revealed that Regions A' and C135 had direct toppling landslide potential, while Regions B140 and C120 had wedge toppling landslide potential. Figure 8 shows the position of the discontinuity plane's line of intersection in Region A' at N196°E/42° in the southwest, about a total criticality of 34 out of 120 or 28.33%; Figure 9 depicts the location of Region B140 at N162°E/9° in the southeast-southeast, alongside a total criticality of 16 out of 45 or 35.56%. Figure 10 represents the total criticality for Region C120 N53°E/57° heading northeast, which is 80 out of 171 or 46.78%, and Figure 11 displays the total criticality for Region C135 N24°E/6° heading northeast, which stands 37 out of 120 or 30.83%.

The regional geological structural conditions in the research area, which constitute normal and reverse faults, are possibly related to the potential for landslides. The main direction of stress in the joints in the study region is northeast to southwest, which is consistent with the primary stress on normal faults, which normally trend northeast to southwest. When a fault moves, this might modify the force acting on the rock, forming joints. Joints may increase the pore water pressure on the rock and create areas of weakness and entryways for water, leading to stress on the slope material and triggering landslides [37].

Slope Stability

The limit equilibrium approach using the Morgenstern Price method, which will result in slope conditions in the study area that are safe and stable regarding a safety factor (SF) value of above 1.25 [38], was employed to assess the degree of slope stability. This non-circular assessment of the findings of kinematic analysis are used to determine slope stability, which can result in direct toppling and wedge toppling, which are probable landslides.

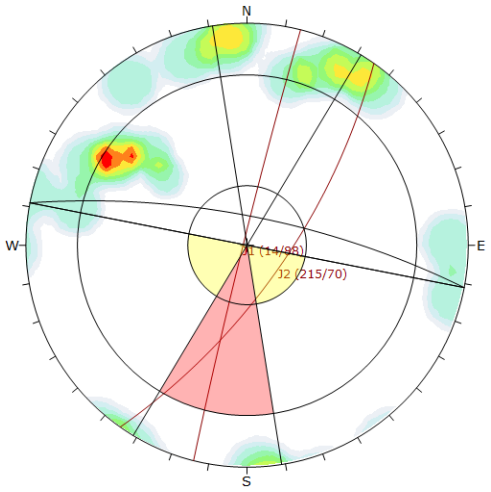


**Figure 8.** Result of kinematic analysis Region A'.

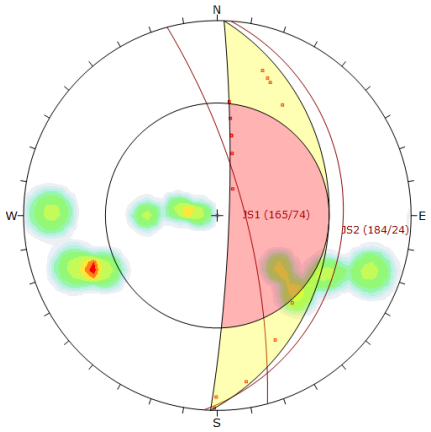


**Figure 9.** Kinematic analysis results Region.

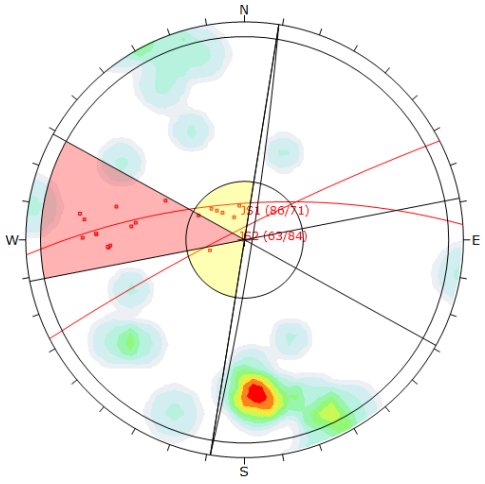


**Figure 10.** Kinematic analysis result Region C120

ISSN : 2085 – 1669
e-ISSN : 2460 – 0288

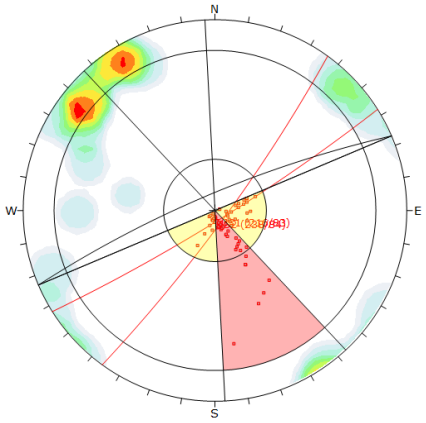


**Figure 11.** Kinematic analysis Region C135

Region A'

SF values under dry and saturated groundwater conditions were obtained in evaluating slope stability measurements for Region A'. Region A' has an SF value of 3.434 in dry groundwater conditions (Figure 12), though it has an SF of 2.358 in saturated groundwater conditions (Figure 13).

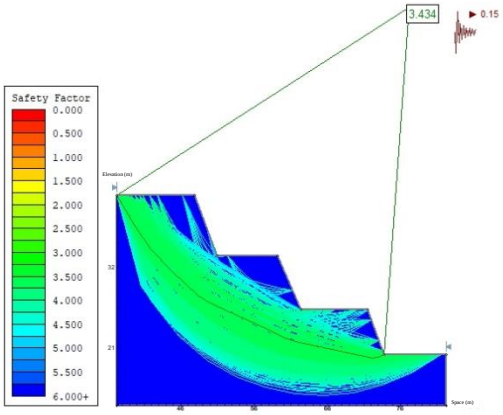


**Figure 12.** Region A' with Dry Conditions, SF 3,434.

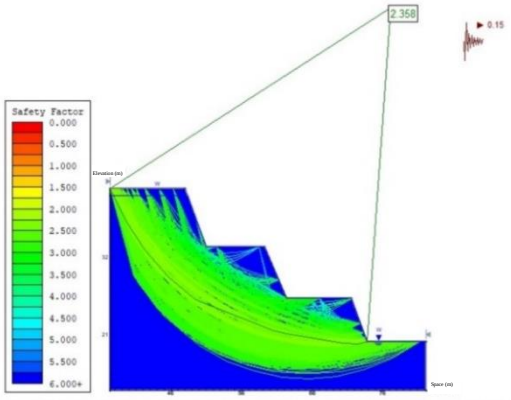


**Figure 13.** Region A' with Saturation Conditions, SF 2,358

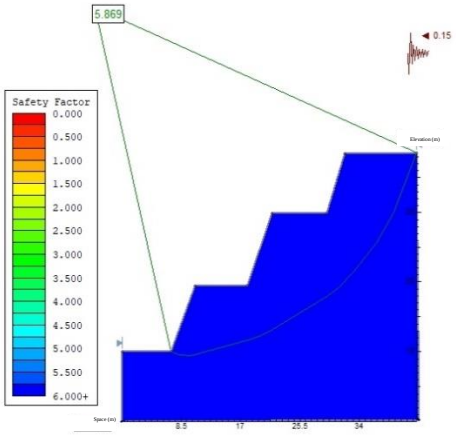


**Figure 14.** Region B140 with Dry Conditions, SF 5,869.

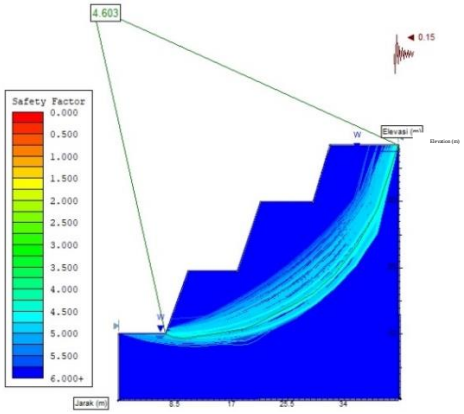


**Figure 15.** Region B140 with Saturation Conditions, SF 4,603

Region B140

SF values for dry and saturated groundwater conditions were obtained in the framework of slope stability measurements for Region B140. Region B140 has an FS value of 5.869 at saturated groundwater conditions and 4.603 for dry groundwater scenarios (see Figures 14 and 15).

Region C120

SF values were obtained for dry and saturated groundwater conditions in examining slope stability data for Region C120. Figure 16 demonstrates that Region C120's SF value is 3.526 in dry groundwater conditions, yet Figure 17 illustrates the value of SF 2.586 in saturated groundwater conditions.

Jurnal Teknologi 16 (1) pp 53-64 © 2024

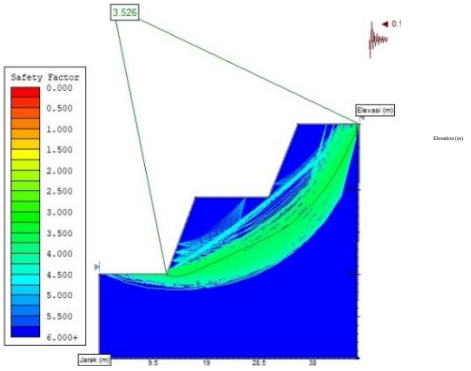


**Figure 16.** Region C120 with Dry Conditions, SF 3,526.

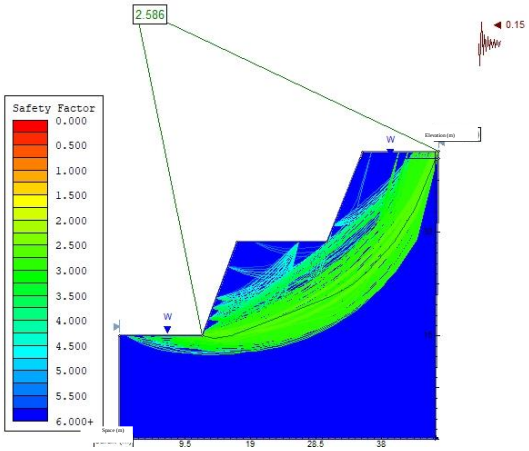


**Figure 17.** Region C120 with Saturation Conditions, SF 2,586

Region C135

SF values were obtained for dry and saturated groundwater conditions in the results of the slope stability examination in Region C135. Region C135 has an SF value of 4.117 in dry groundwater conditions (Figure 18) and an SF value of 3.075 in saturated groundwater conditions (Figure 19).

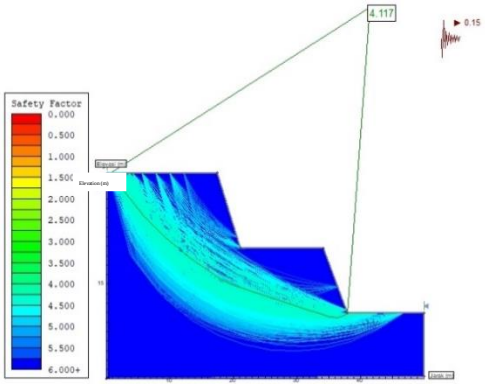


**Figure 18.** Region C135 with Dry Conditions, SF 4,117

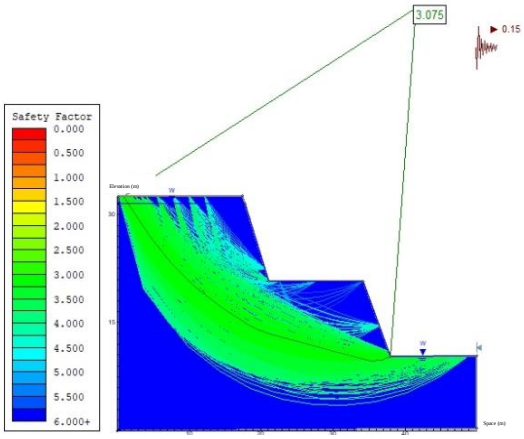


**Figure 19.** Region C135 with Saturation Conditions, SF 3,075.

High SF values imply that the slope stability is safe and stable. Since saturated groundwater generates a lower level of slope stability than dry groundwater, the SF value of a slope in saturated groundwater conditions is lower than the SF value in dry groundwater scenarios. Positive pore water pressure rises in saturated conditions and may lead to slope fall apart [39]. Groundwater has greater effects on slope stability as excavation depth increases.

Slope Geometry Design Recommendation

The slope recommendations are based on actual slope conditions in the four research areas and mining optimizing processes to extract greater reserves by generating safe slope geometric designs. The bench height was determined by mechanical equipment in the subject's area, namely the Excavator PC 750SE-7 with a boom length of 7.1 m and an arm's length of 2.945 m, where the length of the sloping side of the slope is less than 10.045 m. Therefore, the efficient ladder height is 10 m. The width of the bench is selected by business requirements, which is 4 m. At this point, the angle of inclination of a single slope is computed at $80^{o}$ using the greatest SMR value, 79.64. Figures 20 and 21 highlight that the suggested slope yields a lower SF value than the slope SF in actual slope settings, but the conditions are still assessed as safe and stable with SF> 1.25 [38].

ISSN : 2085 – 1669
e-ISSN : 2460 – 0288

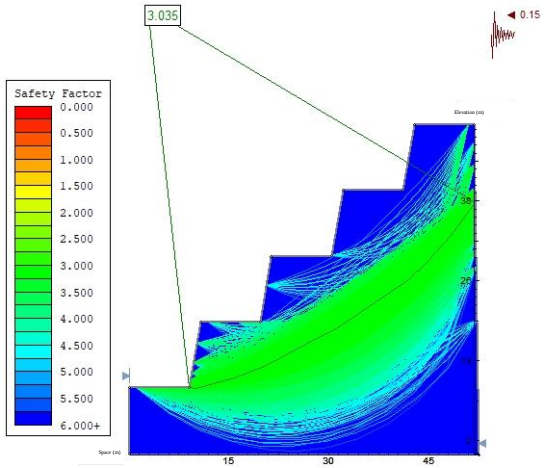


**Figure 20.** Overall Recommended Slope with Dry Conditions, SF 3,035.

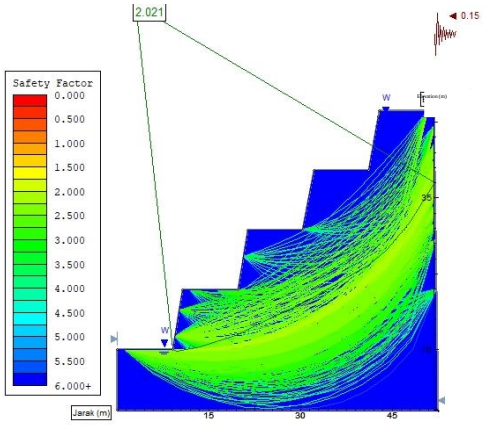


**Figure 21.** Overall Recommended Slope with Saturated Conditions, SF 2,021

## Conclusions

The slope stability analysis using the Morgenstern Price method results in safe and stable slope conditions in the research area, with Region A' getting an SF value of 3,434 in dry groundwater conditions and SF of 2,358 in saturated groundwater conditions, Region B140 with an SF value of 5,869 in dry groundwater conditions and SF 4.603 in saturated groundwater conditions. Region C120 has an SF value of 3.526 in dry groundwater conditions and an SF of 2.586 in saturated groundwater conditions. The overall slope recommendation is a bench height of 10 m, a bench width of 4 m, and a slope angle of 80$^o$, which induces an SF value of 3.035 in dry groundwater conditions and an SF value of 2.021 in saturated groundwater conditions.

## Acknowledgment

The author would like to thank PT Indocement Tunggal Prakarsa Tbk. Plant Cirebon for permitting authors to conduct research in the limestone quarry mining area.

**Funding**
This research received no external funding.

**Author Contributions:** Conceptualization and methodology, H.M.S, N., and Z.H.; software, H.M.S, and Z.H.; validation, N. and Z.H.; formal analysis, H.M.S, N., and Z.H.; investigation, H.M.S, and Z.H.; resources, Z.H.; data curation, N. and Z.H.; writing—original draft preparation, H.M.S; writing—review and editing, H.M.S and N.; visualization, H.L.D.; supervision, Z.H.; project administration, H.M.S. All authors have reviewed and approved the work's published version.

**Conflicts Of Interest**
The authors declare no conflict of interest.

## REFERENCES

[1] Shelley, R.C., Robin, L. dan Plimer, R., (2005). *Encyclopedia of Geology*. United Kingdom: Elsevier Academic Press.

[2] Santika, A. W. dan Mulyadi, D., (2017). Geokimia Batugamping Daerah Montong, Tuban, Jawa Timur. *Riset Geologi dan Pertambangan*, vol. 27, no. 2.

[3] Madiadipoera, T., (1990). *Bahan Galian Industri di Indonesia*. Bandung: Direktorat Jenderal Sumber Daya Mineral Republik Indonesia.

[4] Mossa J, James LA. Impacts of mining on geomorphic systems. In: James LA, Harden C, Clague J, (2013). Geomorphology of human disturbances, climate change, and natural hazards, Treatise on Geomorphology (*J. Shroder, J., Ed. In Chief)*; 2013; 13: p. 74–95.

.[5] Sinha, S. and Banerjee, S. P.(1994). A Method for Estimating Fugitive Particulate Emission from Haul Roads in Opencast Coal Mines and Mitigative Measures, in S. P. Banerjee (ed.), *Proceedings of Second National Seminar on Minerals and Ecology*, Dhanbad, India, pp. 217–227.

[6] Central Mining Research Institute (CMRI). (1998). *Determination of Emission Factor for Various Opencast*

*Mining Activities*, GAP/9/EMG/MOEF/97, Environmental Management Group, Dhanbad, India.

[7] Verma H K, Samadhiya N K, Singh M., Goel R K and Singh P K.(2018). Blast induced rock mass damage around tunnels. *J. Tunneling and Underground Space Technology* 71 149-58. https://doi.org/10.1016/j.tust.2017.08.019

[8] Yamaguchi, U., & Shimotani, T. (1986). A case study of slope failure in a limestone quarry. *International Journal of Rock Mechanics and Mining Science & Geomechanics Abstracts*, 23(1), 95–104. https://doi.org/10.1016/0148-9062(86)91670-0

[9] Harries, N., Noon, D., dan Pritchett, (2009). Slope Stability Radar for Managing Rock Fall Risk in Open Cut Mines. *Proceeding of the 3rd CANUS Rock Mechanics Symposium, Toronto 2009*.

[10] Brady, B. H. G., dan Brown, E. T., (1985). *Rock Mechanics for Underground Mining*. George Allen and Unwin: London.

[11] Sjoberg, J., (1996). *Large Scale Slope Stability in Open Pit Mining – A Review*. Technical Report, Devision of Rock Mechanics, Lulea University of Technology.

[12] Liu,X.R, Xu,B., Liu, Y. Q., Wang,J., and Lin,G. (2020). Cumulative damage and stability analysis of bedding rock slope under frequent microseisms, *Chinese Journal of Geotechnical Engineering*, vol. 42, no. 4, pp. 632–641.

[13] Xu, L. L. Zhang, Q. L. and Feng, R. (2021). Numerical simulation of backfill strength based on optimization of stope structural parameters. *Gold Science and Technology*, vol. 29, no. 3, pp. 421–432.

[14] Jiang, Z. A. , Wang, Y. P. and Men, L. G. (2021). Ventilation control of tunnel drilling dust based on numerical simulation, *Journal of Central South University*, vol. 28.

[15] Tao, Z. G., Zhu, C., He, M. C., and Karakus, M. (2021). A physical modeling-based study on the control mechanisms of Negative Poisson's ratio anchor cable on the stratified toppling deformation of anti-inclined slopes.*International Journal of Rock Mechanics and Mining Sciences*, vol. 138, Article ID 104632. https://doi.org/10.1016/j.ijrmms.2021.104632

[16] Zhu,C., He,M., Karakus,M., Zhang,X., Tao, Z. (2021). Numerical simulations of the failure process of anaclinal slope physical model and control mechanism of negative Poisson's ratio cable, *Bulletin of Engineering Geology and the Environment*, vol. 80, no. 4, pp. 3365–3380.

[17] Wang,Y., Feng, W. K., Hu, R. L. and Li, C. H. (2021). Fracture evolution and energy characteristics during marble failure under triaxial fatigue cyclic and confining pressure unloading (FC-CPU) conditions," *Rock Mechanics and Rock Engineering*, vol. 54, no. 2, pp. 799–818.

[18] Li,B., Bao,R., Wang,Y., Liu,R., and Zhao,C., (2021). Permeability evolution of two-dimensional fracture networks during shear under constant normal stiffness boundary conditions, *Rock Mechanics and Rock Engineering*, vol. 54, no. 3, pp. 1–20.

[19] Bieniawski, Z. T., (1989). *Engineering Rock Mass Classifications*. John-Wiley: New York.

[20] Romana M (1985). New adjustment ratings for application of Bieniawski classification to slopes. In: *proceedings of international symposium on the role of rock mechanics*. Zacatecas, ISRM, pp 49–53.

[21] Kumar M, Rana S, Panta DP, Patel RC. (2017). Slope stability analysis of Balia Nala landslide, Kumaun Lesser Himalaya, Nainital, Uttarakhand, India. *J Rock Mech Geotech Eng* 9:150–158. https://doi.org/10.1016/j.jrmge.2016.05.009

[22] Morales, M., Panthi, K. K. ., Botsialas, K., (2019). Slope stability assessment of an open pit mine using three-dimensional rock mass modeling, *Bull Eng Geol Environ*.78:1249–1264. https://doi.org/10.1007/s10064-017-1175-4

[23] Rusydy, I., Fathani, T.F., Al‐Huda, N., Sugiarto, Iqbal, K., Jamaluddin, K., Meilianda, M., (2021). Integrated approach in studying rock and soil slope stability in a tropical and active tectonic

ISSN : 2085 – 1669
e-ISSN : 2460 – 0288

country, *Environmental Earth Sciences* 80:58 https://doi.org/10.1007/s12665-020-09357-w

[24] Pasha, S. R., Sunarwan, B., dan Syaiful, M., (2018). Analisis Potensi Longsor Menggunakan Metode Kinematik pada Tambang Terbuka *Limestone* Narogong PT Holcim Indonesia Tbk Kecamatan Cileungsi Kabupaten Bogor Jawa Barat. *Jurnal Online Mahasiswa (JOM) Bidang Teknik Geologi*, vol.1, no. 1.

[25] Sirait, B., Pulungan, Z., & Pujianto, E., (2021). Identifikasi potensi longsoran lereng pada kuari batugamping menggunakan analisis kinematika. *Jurnal Teknologi Mineral dan Batubara*, vol. 17, no. 2, hlm. 61-75.

[26] ISRM, (1981). *Rock Characterization Testing and Monitoring ISRM Suggested Method. E.T. Brown (Ed)*. Pergamon Press, hlm. 5 - 30.

[27] Kementerian Pekerjaan Umum. (2017). *Peta Percepatan Puncak di Batuan Dasar (Sb) untuk Probabilitas Terlampau 10% dalam 50 Tahun*.

[28] Badan Standarisasi Nasional. (2010). *SNI 7571 Tahun 2010 Tentang Baku Tingkat Getaran Peledakan pada Kegiatan Tambang Terbuka terhadap Bangunan*.

[29] Shobari, A. F., Mufti, I. J., Khoirullah, N., Zakaria, Z., Sophiana, R. I., dan Mulyo, A. (2019). Hubungan Nilai Koefisien Gempa Horizontal (Kh) dengan Nilai Safety Factor (FS) Daerah Cilengkrang, Jawa Barat. *Padjadjaran Geoscience Journal*, vol. 3, no. 4, hlm. 243 – 253.

[30] Waskita, A. D., Febriadi, A., Rampan, R., Oktavianto, H., dan Patmo, N. (2020). Analisis Kestabilan Lereng Batuan Lunak dengan Model Material Validated Transition pada Rancangan PIT Wara 2020 PT Adaro Indonesia. *Prosiding Temu Profesi Tahunan PERHAPI*, 865-874.

[31] Hoek, E. and Bray, J.W. (1981). Rock Slope Engineering. Revised 3rd Edition, The Institution of Mining and Metallurgy, London, 341-351.

[32] Deere, D. U., dan Deere, D. W., (1989). *Rock Quality Designation (RQD) after Twenty Years*. Deere (Don U) Consultant Gainesville Fl.

[33] Zhang, L., (2016). Determination and applications of rock quality designation (RQD), Journal of Rock Mechanics and Geotechnical Engineering Volume 8, Issue 3, June 2016, Pages 389-397. https://doi.org/10.1016/j.jrmge.2015.11.008

[34] Öge, I.F, (2017). Assessing Rock Mass Permeability Using Discontinuity Properties, Symposium of the International Society for Rock Mechanics, Procedia Engineering 191 ( 2017 ) 638 – 645.https://doi: 10.1016/j.proeng.2017.05.373

[35] Hoek, E. dan Marinos, P., (2000). GSI: a Geologically Friendly Tool for Rock Mass Strength Estimation. *ISRM International Symposium*. OnePetro.

[36] Xing, Y., Kulatilake, P.H.S.W., Sandbak, L.A. (2018). Effect of rock mass and discontinuity mechanical properties and delayed rock supporting on tunnel stability in an underground mine, *Engineering Geology* Volume 238, 2 May 2018, Pages 62-75. https://doi.org/10.1016/j.enggeo.2018.03.010

[37] Guerriero, L., Prinzi, E.P., Calcaterra, D., Ciarcia, S., Di Martire, D., Guadagno, F.M., Ruzza, G., Revellino, P., (2021). Kinematics and geologic control of the deep-seated landslide affecting the historic center of Buonalbergo, southern Italy, *Geomorphology* Volume 394, 1 December 2021, 107961. https://doi.org/10.1016/j.geomorph.2021.107961.

[38] Bowles, J. E., (1984). *Physical and Geotechnical Properties of Soil: Second Edition*. McGraw-Hill: New York, USA.

[39] Acharya, K.P.; Netra, P.B.; Ranjan, K.D.; Ryuichi, Y.(2016). Seepage and slope stability modelling of rainfall-induced slope failures in topographic hollows. *Geomat. Nat. Hazards Risk* 7, 721–746. https://doi.org/10.1080/19475705.2014.954150